New Direct Torque and Flux Control with Improved Torque per Ampere for Switched Reluctance Motor

Krishna Reddy Pittam†, *Student Member*, *IEEE*, Deepak Ronanki‡, *Student Member*, *IEEE*,
Parthiban Perumal†, *Senior Member*, *IEEE* and Sheldon S. Williamson‡, *Senior Member*, *IEEE*
†Dept. of Electrical and Electronics Engineering, National Institute of Technology Karnataka, Karnataka-575025, India
‡Dept. of Electrical and Computer Engineering, University of Ontario Institute of Technology, ON L1G 0C5, Canada
Email: krishnareddy4308@gmail.com, dronanki@ieee.org, parthiban@nitk.edu.in and sheldon.williamson@uoit.ca

***Abstract*—Inherent torque ripple, acoustic noise and vibration are the major hindrances of switched reluctance motor (SRM) for wide acceptance in the automotive industry. To avoid stability issues in electrified vehicles, smooth torque control of an SRM is requisite. Torque ripple in the SRM can be avoided by proper machine design and/or directly controlling the torque. To maintain the torque within the hysteresis band in the conventional direct torque and flux control (DTFC), a high value of RMS current flows through the motor windings. This results in an increase in copper losses and reduces the net torque per ampere ratio. This paper addresses this issue by proposing a new DTFC technique for an SRM drive with the features of improved torque per ampere while maintaining the torque within the hysteresis bands. MATLAB simulations show that the proposed DTFC technique enhances torque per ampere ratio while minimizing the torque ripple. The effectiveness of the proposed DTFC strategy is also demonstrated through real-time simulations in the OPAL-RT digital platform. Real-time results show that the proposed DTFC strategy exhibits better performance in comparison to the conventional DTFC under steady-state and dynamic conditions.**

***Index Terms*—Motor drives, switched reluctance motor, torque control, traction motors and torque ripple minimization.**

I. Introduction

In recent years, the development of electric vehicles (EVs) has gained attention due to increased concerns regarding environmental pollution and energy crisis. To meet the required demand, electric motors form a main energy conversion system which needs to satisfy the performance as well as safety requirements [1], [2]. Primarily, the automotive market is dominant with permanent magnet synchronous motors (PMSM) due to superior power density and efficiency over a wide torque-speed range [3]. However, price volatility and non-availability of rare-earth materials used in PMSMs has caused an increased interest in developing permanent magnetless motor drive topologies that are more reliable and efficient [4].

Among them, switched reluctance motor (SRM) is the most prominent magnet-free motor topology due to its robust electromechanical structure, wide speed-torque region, high starting torque, no shoot-through converter fault and low-cost [5], [6]. Moreover, it also enables fault-tolerant operation. However, the utilization of SRM is limited in the automotive industry due to inherent torque ripple, the requirement of precise rotor position information, acoustic noise and vibration. Furthermore, smooth torque control is intractable due to non-linear magnetic and torque characteristics of the SRM [7]. Therefore, there is ongoing research of control of SRM with minimal torque pulsations in EVs.

Over the past years, many research investigations have been carried out to minimize the torque ripple, which is mainly classified based on machine design optimization and control approaches. Minimization of torque ripple through machine design involves the optimization of machine parameters such as pole shape, air gap, core, winding arrangement and geometry modifications [8]–[13]. In addition, an increase in phase number has an added advantage in terms of torque ripple and fault-tolerance. For instance, torque ripple in the four-phase SRMs is lesser than three-phase SRMs. However, a further increase in phase number increases the device component count, thus increasing the system cost and complicating the control algorithms. Therefore, four-phase SRMs are widely accepted in the various industrial and electric transportation applications [14].

On other hand, torque ripple can be reduced using optimized control techniques such as current/flux profiling techniques (CPT) [15], [16] and torque sharing functions (TSFs) [17]–[19], where the torque is an indirect control variable. However, these approaches require optimal tuning of control parameters, off-line calculations and consumes memory in the digital controllers to store pre-defined characteristics. Alternatively, torque is directly controlled through direct instantaneous torque control (DITC) [20], [21], direct average torque control (DATC) [22], direct torque and flux control (DTFC) [23], [24] and model predictive control strategies [25]. The performance comparison of different control strategies such as CPT, TSFs, DITC and DTFC are studied and merits and demerits of each method is well established in the literature [26]–[28].

The DTFC scheme [23] draws significant interest as it uses the direct torque control (DTC) concept of conventional AC motors. This method avoids determination of the turn-on, and off angles, fast transient response, insensitive to motor parameters, reduced vibration, and the possibility for sensorless operation [26]. In this strategy, the movement of the flux linkage vector enables the direct control of the phase torque, where the magnitude of resultant flux vector is maintained within a hysteresis band. However, higher positive torque must be produced by active phase during commutation of outgoing phase, thereby drawing higher source current [26], [27]. As a result, there is a reduction in overall torque per ampere and

978-1-5386-9350-6/19/$31.00 ©2019 IEEE

the efficiency of the SRM drive.

In this paper, a new DTFC method for four-phase SRM is proposed to improve torque per ampere ratio. In this method, a new switching sequence is developed by partitioning into sixteen sector regions and optimized voltage vectors are selected in such a way that the current of outgoing phase is made to decay quickly while maintaining smooth control of active phase to generate the desired torque. Therefore, conduction time of each phase is reduced and the desired torque is maintained. As a result, the proposed strategy not only minimizes the torque ripple but also reduces the copper losses and improves the torque per ampere ratio. The efficacy of the proposed DTFC strategy is validated on a 4-kW four-phase SRM through MATLAB simulations and verified on a real time digital simulator using OPAL-RT. The results show the improved performance of the proposed DTFC strategy in comparison with the conventional DTFC scheme.

II. Switched Reluctance Motor Drive

A dynamic model of an SRM can be represented with a set of electrical equations for each phase and the dynamics of the system. The voltage equation of an m-phase machine without considering mutual coupling can be expressed as

$$v_j = r_j \cdot i_j + \frac{d\psi_j(i_j,\theta_j)}{dt}; j \ = \ 1, 2..... \ m \tag{1}$$

where v_j, i_j, r_j, ψ_j and θ_j represents terminal voltage, phase current, phase winding resistance, flux linkages and rotor position of "j" phase respectively.

$$v_j = r_j \cdot i_j + \frac{\partial \psi_j}{\partial i_j} \cdot \frac{di_j}{dt} + \frac{\partial \psi_j}{\partial \theta_j} \cdot \frac{d\theta_j}{dt} \tag{2}$$

The dynamic equation of the phase current can be expressed as

$$\frac{di_j}{dt} = \left[\frac{\partial \psi_j}{\partial i_j}\right]^{-1} \cdot \left[v_j - r_j \cdot i_j - \frac{\partial \psi_j}{\partial \theta_j} \cdot \omega\right] \tag{3}$$

where $\omega = \frac{d\theta}{dt}$ is rotor speed.

The dynamic equations of the mechanical system can be expressed as

$$\sum_{j=1}^{m} T_j(i_j,\theta_j) - T_L = J \cdot \frac{d\omega}{dt} + B \cdot \omega \tag{4}$$

The speed equation can be rewritten as

$$\frac{d\omega}{dt} = \frac{1}{J}\left[\sum_{j=1}^{m} T_j(i_j,\theta_j) - T_L - B \cdot \omega\right] \tag{5}$$

In general, the instantaneous torque per phase at any position can be expressed as

$$T_j = \left.\frac{\partial W_c(i_j,\theta)}{\partial \theta}\right|_{i_j = constant} \tag{6}$$

where $W_c(i_j,\theta)$ denotes co-energy, which can be given by

$$W_c = \int_0^i \psi(i,\theta) di \tag{7}$$

The average torque expression over a time interval T can be obtained as

$$T_{avg} = \frac{1}{T}\int_0^T \left(\sum_{j=1}^{m} T_j(i_j,\theta_j)\right) dt \tag{8}$$

Torque ripple can be defined as

$$T_{ripple} = \frac{T_{max} - T_{min}}{T_{avg}} \times 100\% \tag{9}$$

The SRM usually operates in the saturation mode to achieve high energy conversation rate, which makes a highly non-linear machine and difficult to control. Thus, it is essential to develop non-linear SRM model for high-performance control techniques. A non-linear model of an SRM is developed using electromagnetic (flux and torque) characteristics [29] as shown in Fig. 1.

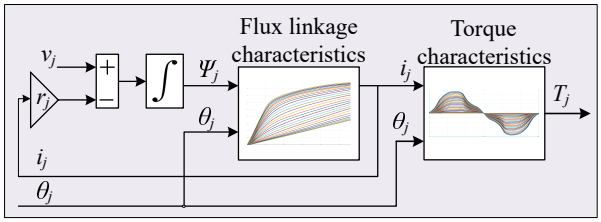

Fig. 1. A non-linear per-phase model of an SRM.

Several inverter power circuits have been proposed in the literature to control SRM with unipolar current [30]. Among them, asymmetric H-bridge converter (AHB) is the most widely used power converter topology to drive the SRM as it allows independent control of each phase. Fig. 2 shows the electric circuit of AHB converter for a four-phase SRM. Each H-bridge converter is used to drive the one-phase of the SRM. This converter comprises of two power switching devices and diodes per phase, and the phase winding is connected in series with the power switches. There are three possible states that

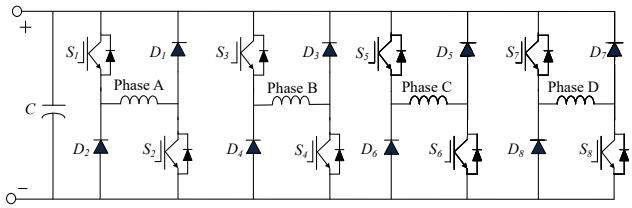

Fig. 2. Asymmetric bridge converter for four-phase SRM.

can be achieved through asymmetric bridge converter to drive the SRM. The possible voltage states for phase-A is defined as:

- Magnetizing state (+V_{dc}): S_1 = 1 and S_2 = 1 (+1)
- Freewheeling state (0): S_1 = 0 and S_2 = 1 or S_1 = 1 and S_2 = 0 (0)
- Demagnetizing state (-V_{dc}): S_1 = 0 and S_2 = 0 (-1)

III. Proposed Direct Torque and Flux Control

The DTFC scheme [23] of an SRM is derived from DTC philosophy utilized for AC machines. In this strategy, the magnitude of stator flux linkage and electro-magnetic torque are maintained in the hysteresis band by decelerating or accelerating the stator-flux vector based on decrement and increment of the electro-magnetic torque. This scheme does

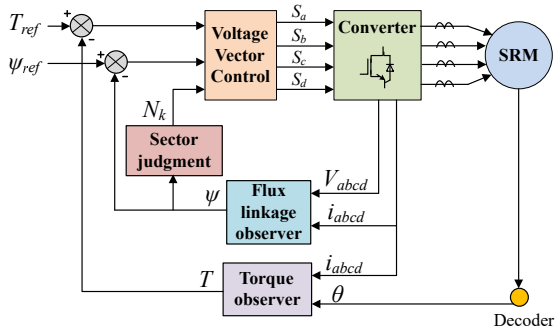

Fig. 3. Block diagram of DTFC scheme for four-phase SRM.

not require any motor information as the torque control depends only on the stator flux vector's variation. The control block diagram of an SRM using the DTFC strategy is shown in Fig. 3. The DTFC controller requires flux-linkage error, torque error and a flux-linkage vector's position information to choose optimized voltage vector such that the smooth torque control of an SRM drive is achieved. In this method, total electrical

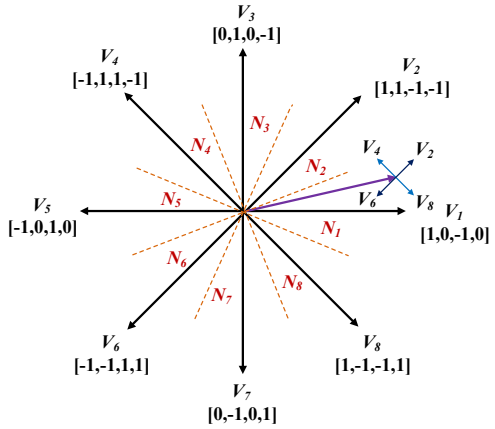

Fig. 4. Definitions of voltage vectors and eight sectors for the conventional DTFC scheme.

space is divided into eight sectors with an angle of 45^o. The DTFC controller chooses switching table shown in Table I and selects the suitable voltage vector to reduce torque and flux errors, as shown in Fig. 4. The stator phase flux-linkage can be estimated using stator voltages and currents as

$$\psi_j = \int_0^t (v_j - r_j \cdot i_j) \cdot dt + \psi_{jo} \tag{10}$$

In SRM, the phase current and flux returns to zero in each electrical cycle, thus $\psi_{jo} = 0$.

TABLE I
Switching Table for the Conventional DTFC

Sector	$T\uparrow \psi\uparrow$	$T\uparrow \psi\downarrow$	$T\downarrow \psi\uparrow$	$T\downarrow \psi\downarrow$
N_1	V_2	V_4	V_8	V_6
N_2	V_3	V_5	V_1	V_7
N_3	V_4	V_6	V_2	V_8
N_4	V_5	V_7	V_3	V_1
N_5	V_6	V_8	V_4	V_2
N_6	V_7	V_1	V_5	V_3
N_7	V_8	V_2	V_6	V_4
N_8	V_1	V_3	V_7	V_5

To evaluate the single stator flux linkage vector, the flux vectors for four-phase SRM are transformed to a stationary orthogonal $(\alpha - \beta)$ reference axes

$$\overrightarrow{\psi_s} = \overrightarrow{\psi_\alpha} + j\overrightarrow{\psi_\beta} \tag{11}$$

$$\left.\begin{aligned} |\psi_s| &= \sqrt{\psi_\alpha^2 + \psi_\beta^2} \\ \delta &= tan^{-1}(\tfrac{\psi_\beta}{\psi_\alpha}) \end{aligned}\right\} \tag{12}$$

where $|\psi_s|$ is the magnitude of flux-linkage vector and δ is the flux vector angle, which is used to determine the sector N_k $(k \in \{1, 2, ..., 8\})$. To maintain the torque within hysteresis

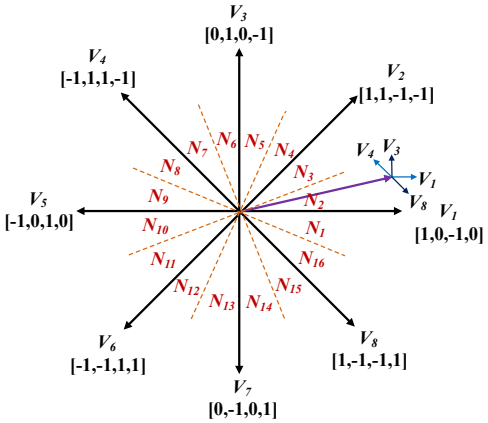

Fig. 5. Definitions of voltage vectors and sixteen sectors for the proposed DTFC scheme.

bands, the DTFC controller requires torque feedback which can be achieved through pre-determined torque characteristics of the motor. However, the higher positive torque has to be produced by active phase during commutation of outgoing phase, thereby draws higher current from the source. This is due to the existence of phase current in the negative inductance slope region (negative torque production region) and dead zone (zero torque production region). As a result, the efficiency of the SRM drive decreases.

To overcome this problem, a new DTFC scheme is introduced, which reshapes the current waveform to improve torque per ampere ratio with new voltage vector selection. In this

TABLE II
SWITCHING TABLE FOR THE PROPOSED DTFC

Sector	$T\uparrow \psi\uparrow$	$T\uparrow \psi\downarrow$	$T\downarrow \psi\uparrow$	$T\downarrow \psi\downarrow$
N_1	V_2	V_3	V_8	V_7
N_2	V_3	V_4	V_1	V_8
N_3	V_3	V_4	V_1	V_8
N_4	V_4	V_5	V_2	V_1
N_5	V_4	V_5	V_2	V_1
N_6	V_5	V_6	V_3	V_2
N_7	V_5	V_6	V_3	V_2
N_8	V_6	V_7	V_4	V_3
N_9	V_6	V_7	V_4	V_3
N_{10}	V_7	V_8	V_5	V_4
N_{11}	V_7	V_8	V_5	V_4
N_{12}	V_8	V_1	V_6	V_5
N_{13}	V_8	V_1	V_6	V_5
N_{14}	V_1	V_2	V_7	V_6
N_{15}	V_1	V_2	V_7	V_6
N_{16}	V_2	V_3	V_8	V_7

scheme, the phase current is restricted to enter into the dead zone with an appropriate voltage vector selection based on the location of the reference vector. To realize the optimized voltage vector selection, sixteen sector partition method with an electrical angle of 22.5^o is employed instead of the eight sector approach as in the conventional DTFC scheme. The sixteen sector partition approach allows the precise selection of voltage vectors corresponding to torque and flux errors. Furthermore, the voltage vectors at $+90^o$ and -90^o are selected to increase the torque ($T\uparrow$) and decrease the torque ($T\downarrow$) to achieve a faster dynamic response, which is not possible in the conventional DTFC scheme as each sector occupies 45^o of rotor position. In the proposed DTFC scheme, each sector N_k ($k \epsilon \{1, 2, ..., 16\}$) covers only 22.5^o which allows the change of vector selection for each 22.5^o that doubles the chances to select the optimized voltage vectors when compared with conventional DTFC scheme. Therefore, the proposed DTFC method selects the most appropriate voltage vector to the maximum extent so as to improve the dynamic response as well as torque per ampere. The vector diagram of voltage vector selection with sixteen sector partition for proposed DTFC is shown in Fig. 5 and their corresponding switching table is listed in Table II.

IV. RESULTS AND DISCUSSION

To validate the performance and effectiveness of the proposed DTFC scheme, detailed simulation studies have been carried out on 4-kW four-phase SRM. The magnetization and static characteristics can be obtained either by finite element (FE) analysis or experimental measurement. The characteristics obtained from experimental measurements are more suitable for modelling of SRM as it is more accurate than FE analysis because FE analysis excludes some complex secondary effects. In this study, a non-linear dynamic model of SRM is developed using the flux and torque characteristics of a real SR machine in the form of two-dimensional (2D) lookup tables. As discussed in Section II and III, the SRM model and its DTFC controller are developed in MATLAB/SIMULINK platform.

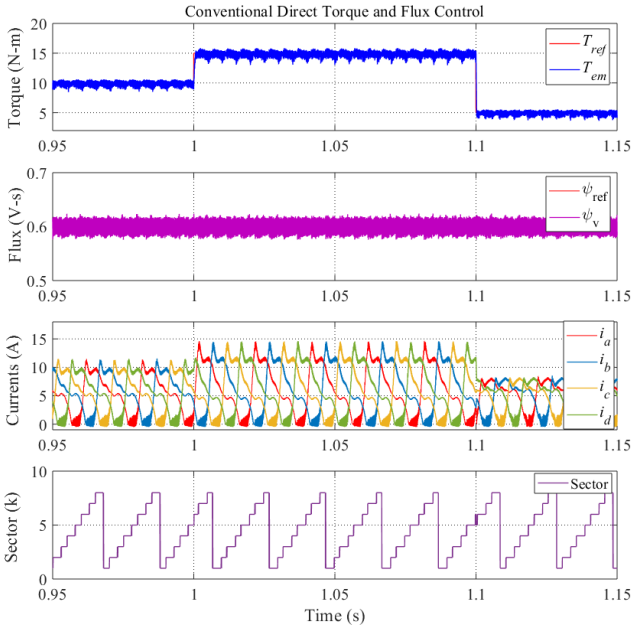

Fig. 6. Simulation results of the conventional DTFC scheme under step change in torque references at 500 rpm.

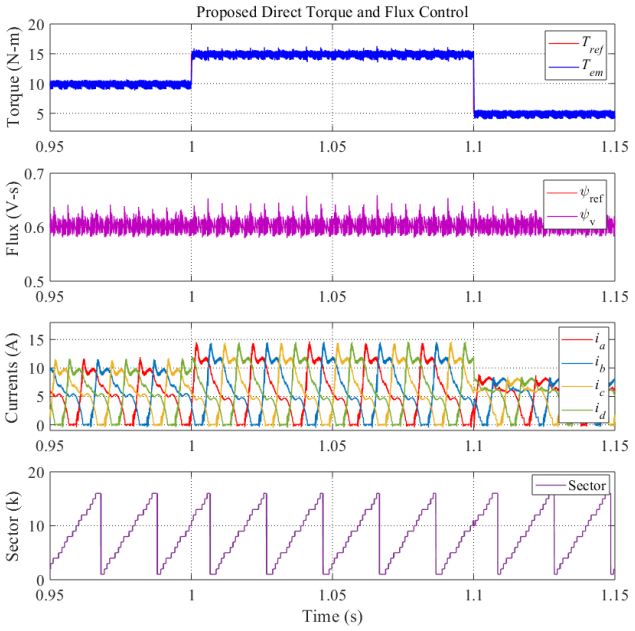

Fig. 7. Simulation results of the proposed DTFC scheme under step change in torque references at 500 rpm.

Figs. 6 and 7 show the simulated waveforms of the conventional DTFC and the proposed DTFC schemes under different torque references at 500 rpm respectively. It is noticed that

TABLE III
PERFORMANCE COMPARISON BETWEEN THE PROPOSED DTFC AND THE CONVENTIONAL DTFC AT 500 RPM

Parameter	Conventional DTFC			Proposed DTFC		
Reference torque (N-m)	T_{ref} = 5	T_{ref} = 10	T_{ref} = 15	T_{ref} = 5	T_{ref} = 10	T_{ref} = 15
Torque ripple (%)	38.41	23.10	19.21	33.07	19.01	18.53
Torque per ampere (N-m/A)	0.832	1.315	1.528	1.107	1.591	1.762

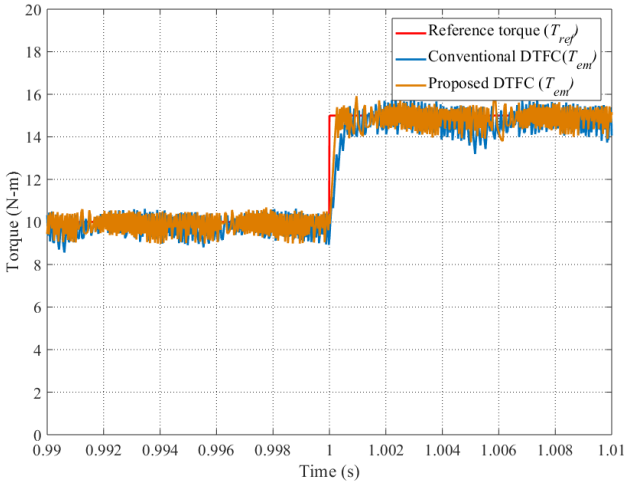

Fig. 8. Transient response of an SRM drive during acceleration.

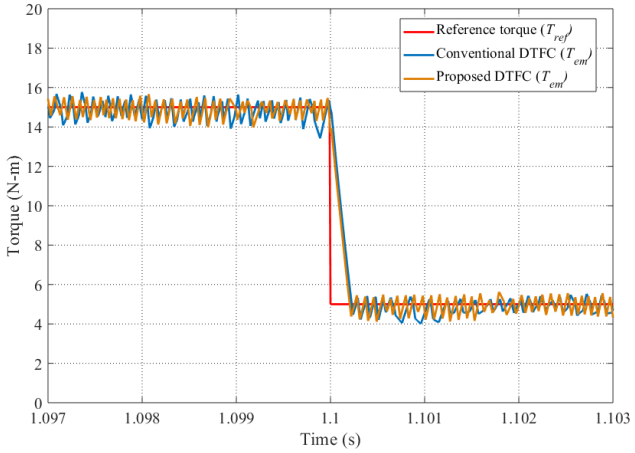

Fig. 9. Transient response of an SRM drive during deceleration.

both flux and torque are well controlled at their reference values using the proposed DTFC strategy and outperforms the conventional DTFC strategy in terms of torque ripple minimization and improving torque per ampere. It is known that flux vector information in the DTFC scheme is enough for the sensorless operation, the prediction error can be minimized using the proposed DTFC scheme due to more sector partition as shown in Fig. 7. Furthermore, the dynamic response of the proposed scheme is evaluated under step change in the torque references during acceleration and declaration drive modes. The results of SRM drive under step change in torque

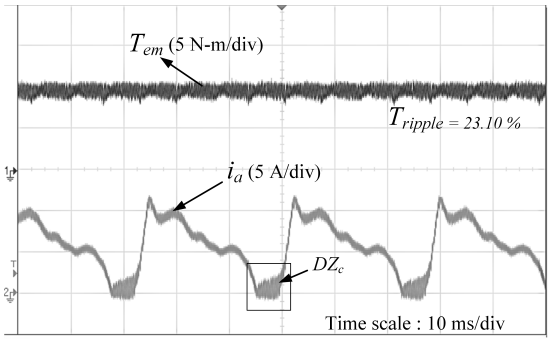

Fig. 10. Real-time results of the conventional DTFC at 500 rpm: : CH1: Torque (N-m) and CH2: Phase-A current (A); Time scale: 10 ms/div.

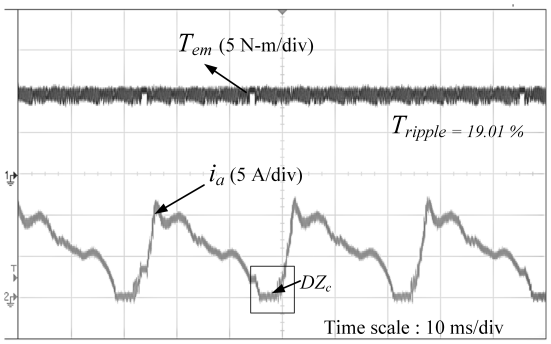

Fig. 11. Real-time results of the proposed DTFC at 500 rpm : CH1: Torque (N-m) and CH2: Phase-A current (A); Time scale: 10 ms/div.

reference from 10 N-m to 15 N-m and 15 N-m to 5 N-m are shown in Figs. 8 and 9 respectively. A fast dynamic response is observed under step change in torque references during both the conditions in case of the proposed DTFC scheme. This shows the proposed DTFC scheme exhibits better performance under steady-state and dynamic operating conditions.

Furthermore, real-time simulation studies are conducted in a digital simulator to verify the effectiveness of the proposed scheme. The real-time results of the conventional DTFC and the proposed DTFC are shown in Figs. 10 and 11 respectively. The elimination of the phase current using the proposed DTFC scheme especially in the dead zone (DZ) region is observed in comparison to the conventional DTFC scheme, thereby draws less source current and improves torque per ampere in the SRM drive using the proposed DTFC. Furthermore, the torque ripple is also minimized. The comparison between these methods in terms of torque ripple and torque per ampere is

listed in Table III. From the analysis, it is concluded that the proposed scheme outperforms under steady-state and dynamic conditions in comparison to the conventional DTFC schemes.

V. Conclusion

In this paper, a new DTFC scheme with improved torque per ampere in a SRM drive for vehicular applications is reported. In this technique, the voltage vectors are selected to minimize torque ripple as well as to increase torque per ampere ratio. A 4-kW 8/6-pole four-phase SRM drive system is used to verify the effectiveness of the proposed method through MATLAB simulations. The performance of this technique is also compared with the conventional DTFC strategy. Finally, the proposed DTFC strategy is verified on a real-time digital simulator using OPAL-RT. Results confirm that the proposed methodology not only displays a good dynamic performance but also improves the torque per ampere ratio as well as reducing the torque ripples under steady-state operation.

References

[1] B. Bilgin et al., "Making the Case for Electrified Transportation," *IEEE Trans. Transport. Electrific.*, vol. 1, no. 1, pp. 4-17, June 2015.

[2] D. Ronanki and P. Perumal, "A Small 4-wheeler EV Propulsion System Using DTC Controlled Induction Motor," in *Proc. World Congress on Engineering*, vol. 2, London, UK, July 2013.

[3] Y. Yang et al., "Design and Comparison of Interior Permanent Magnet Motor Topologies for Traction Applications," *IEEE Trans. Transport. Electrific.*, vol. 3, no. 1, pp. 86-97, March 2017.

[4] I. Boldea, L. N. Tutelea, L. Parsa and D. Dorrell, "Automotive Electric Propulsion Systems With Reduced or No Permanent Magnets: An Overview," *IEEE Trans. Ind. Electron.*, vol. 61, no. 10, pp. 5696-5711, Oct. 2014.

[5] Z. Yang, F. Shang, I. P. Brown and M. Krishnamurthy, "Comparative Study of Interior Permanent Magnet, Induction, and Switched Reluctance Motor Drives for EV and HEV Applications," *IEEE Trans. Transport. Electrific.*, vol. 1, no. 3, pp. 245-254, Oct. 2015.

[6] A. Chiba, K. Kiyota, N. Hoshi, M. Takemoto and S. Ogasawara, "Development of a Rare-Earth-Free SR Motor With High Torque Density for Hybrid Vehicles," *IEEE Trans. Energy Convers.*, vol. 30, no. 1, pp. 175-182, March 2015.

[7] E. Bostanci, M. Moallem, A. Parsapour and B. Fahimi, "Opportunities and Challenges of Switched Reluctance Motor Drives for Electric Propulsion: A Comparative Study," *IEEE Trans. Transport. Electrific.*, vol. 3, no. 1, pp. 58-75, March 2017.

[8] Y. K. Choi, H. S. Yoon and C. S. Koh, "Pole-Shape Optimization of a Switched-Reluctance Motor for Torque Ripple Reduction," *IEEE Trans. Magn.*, vol. 43, no. 4, pp. 1797-1800, April 2007.

[9] S. I. Nabeta, I. E. Chabu, L. Lebensztajn, D. A. P. Correa, W. M. da Silva and K. Hameyer, "Mitigation of the Torque Ripple of a Switched Reluctance Motor Through a Multiobjective Optimization," *IEEE Trans. Magn.*, vol. 44, no. 6, pp. 1018-1021, June 2008.

[10] G. Li, J. Ojeda, S. Hlioui, E. Hoang, M. Lecrivain and M. Gabsi, "Modification in Rotor Pole Geometry of Mutually Coupled Switched Reluctance Machine for Torque Ripple Mitigating," *IEEE Trans. Magn.*, vol. 48, no. 6, pp. 2025-2034, June 2012.

[11] V. Rallabandi and B. G. Fernandes, "Design Methodology for High-Performance Segmented Rotor Switched Reluctance Motors," *IEEE Trans. Energy Convers.*, vol. 30, no. 1, pp. 11-21, March 2015.

[12] C. Ma and L. Qu, "Multiobjective Optimization of Switched Reluctance Motors Based on Design of Experiments and Particle Swarm Optimization," *IEEE Trans. Energy Convers.*, vol. 30, no. 3, pp. 1144-1153, Sept. 2015.

[13] B. Anvari, H. A. Toliyat and B. Fahimi, "Simultaneous Optimization of Geometry and Firing Angles for In-Wheel Switched Reluctance Motor Drive," *IEEE Trans. Transport. Electrific.*, vol. 4, no. 1, pp. 322-329, March 2018.

[14] S. Xu, H. Chen, F. Dong and J. Yang, "Reliability Analysis on Power Converter of Switched Reluctance Machine System under Different Control Strategies," *IEEE Trans. Ind. Electron.*, to be published, doi: 10.1109/TIE.2019.2892675.

[15] J. Y. Chai and C. M. Liaw, "Reduction of speed ripple and vibration for switched reluctance motor drive via intelligent current profiling," *IET Electric Power Appli.*, vol. 4, no. 5, pp. 380-396, May 2010.

[16] R. Mikail, I. Husain, Y. Sozer, M. S. Islam and T. Sebastian, "Torque-Ripple Minimization of Switched Reluctance Machines Through Current Profiling," *IEEE Trans. Ind. Appl.*, vol. 49, no. 3, pp. 1258-1267, May-June 2013.

[17] X. D. Xue, K. W. E. Cheng and S. L. Ho, "Optimization and Evaluation of Torque-Sharing Functions for Torque Ripple Minimization in Switched Reluctance Motor Drives," *IEEE Trans. Power Electron.*, vol. 24, no. 9, pp. 2076-2090, Sept. 2009.

[18] J. Ye, B. Bilgin and A. Emadi , "An Offline Torque Sharing Function for Torque Ripple Reduction in Switched Reluctance Motor Drives," *IEEE Trans. Power Electron.*, vol. 30, no. 2, pp. 726-735, June 2015.

[19] H. Li, B. Bilgin and A. Emadi, "An Improved Torque Sharing Function for Torque Ripple Reduction in Switched Reluctance Machines," *IEEE Trans. Energy Convers.*, vol. 34, no. 2, pp. 1635-1644, Feb. 2019.

[20] R. B. Inderka and R. W. A. A. De Doncker, "DITC-direct instantaneous torque control of switched reluctance drives," *IEEE Trans. Ind. Appl.*, vol. 39, no. 4, pp. 1046-1051, July-Aug. 2003.

[21] S. Yao and W. Zhang, "A Simple Strategy for Parameters Identification of SRM Direct Instantaneous Torque Control," *IEEE Trans. Power Electron.*, vol. 33, no. 4, pp. 3622-3630, April 2018.

[22] R. B. Inderka and R. W. A. A. De Doncker, "High-dynamic direct average torque control for switched reluctance drives," *IEEE Trans. Ind. Appl.*, vol. 39, no. 4, pp. 1040-1045, July-Aug. 2003.

[23] A. D. Cheok and Y. Fukuda, "A new torque and flux control method for switched reluctance motor drives," *IEEE Trans. Power Electron.*, vol. 17, no. 4, pp. 543-557, July 2002.

[24] D. Ronanki and P. Parthiban, "PV-Battery Powered Direct Torque Controlled Switched Reluctance Motor Drive," in *Proc. IEEE Asia-Pacific Power and Energy Eng. Conf.*, Shanghai, 2012, pp. 1-4.

[25] C. Li, G. Wang, Y. Li and A. Xu, "An improved finite-state predictive torque control for switched reluctance motor drive," *IET Electric Power Appl.*, vol. 12, no. 1, pp. 144-151, 2018.

[26] D. Ronanki and S. S. Williamson, "Comparative analysis of DITC and DTFC of switched reluctance motor for EV applications," in *Proc. IEEE Int. Conf. on Ind. Tech. (ICIT)*, Toronto, ON, 2017, pp. 509-514.

[27] S. Sau, R. Vandana and B. G. Fernandes, "A new direct torque control method for switched reluctance motor with high torque/ampere," in *Proc. 39th Annu. Conf. of the IEEE Ind. Electron. Soc.*, Vienna, 2013, pp. 2518-2523.

[28] A. Pop, V. Petrus, C. S. Martis, V. Iancu and J. Gyselinck, "Comparative study of different torque sharing functions for losses minimization in Switched Reluctance Motors used in electric vehicles propulsion," in *Proc. IEEE Int. Conf. on Optimization of Electrical and Electronic Equipment (OPTIM)*, Brasov, 2012, pp. 356-365.

[29] P. Chancharoensook and M. F. Rahman, "Dynamic modeling of a four-phase 8/6 switched reluctance motor using current and torque look-up tables," in *Proc. 28th Annu. Conf. of the IEEE Ind. Electron. Soc.*, Sevilla, 2002, pp. 491-496.

[30] M. Pittermann, J. Fort, J. Diesl and V. Pavlicek, "Converters for Switched Reluctance Motor - Topology Comparison," in *Proc. Int. Conf. on Mechatronics - Mechatronika (ME)*, Brno, Czech Republic, 2018, pp. 1-8.